

LETTER • OPEN ACCESS

European heatwave tracks: using causal discovery to detect recurring pathways in a single-regional climate model large ensemble

To cite this article: A Böhnisch *et al* 2023 *Environ. Res. Lett.* **18** 014038

View the [article online](#) for updates and enhancements.

You may also like

- [Quantifying impact-relevant heatwave durations](#)
Kelley De Polt, Philip J Ward, Marleen de Ruyter *et al.*
- [Enhanced nighttime heatwaves over African urban clusters](#)
Eghosa Igun, Xiyun Xu, Zitong Shi *et al.*
- [Interactive influence of ENSO and IOD on contiguous heatwaves in Australia](#)
P Jyoteeshkumar Reddy, Sarah E Perkins-Kirkpatrick and Jason J Sharples

ENVIRONMENTAL RESEARCH
LETTERS

LETTER

European heatwave tracks: using causal discovery to detect recurring pathways in a single-regional climate model large ensemble

OPEN ACCESS

RECEIVED
20 August 2022REVISED
24 November 2022ACCEPTED FOR PUBLICATION
8 December 2022PUBLISHED
13 January 2023

Original Content from
this work may be used
under the terms of the
[Creative Commons
Attribution 4.0 licence](#).

Any further distribution
of this work must
maintain attribution to
the author(s) and the title
of the work, journal
citation and DOI.

A Böhnisch^{1,*} , E Felsche^{1,2} and R Ludwig¹¹ Department of Geography, Ludwig-Maximilians University Munich, Luisenstrasse 37, Munich, Germany² Center for Digital Technology and Management, Munich, Germany

* Author to whom any correspondence should be addressed.

E-mail: a.boehnisch@lmu.de**Keywords:** heatwaves, heatwave tracks, SMILE, spatio-temporal propagation, causal discovery, large ensembleSupplementary material for this article is available [online](#)**Abstract**

Summer heatwaves repeatedly affect extended regions in Europe, resulting in adverse economic, social, and ecological impacts. Recent events, e.g. the 2022 heatwave, also attract interest regarding the spatial shifts of their impact centers. Evaluations so far either investigated heatwave passages at pre-defined locations or employed algorithms to spatio-temporally track their core regions. Usually, the latter focus on single events, and thus often fail to generalize spatial heatwave tracks or ignore track characteristics. Here, we use a data-driven approach employing causal discovery to robustly characterize European heatwave tracks in single-model initial condition large ensemble (SMILE) climate simulations to overcome sampling uncertainties of observational records. This enables us to identify specific recurrent heatwave tracks, evaluate their preferential seasonal occurrence, and associate them with moving high pressure centers. Additionally, the evaluation of heatwave track representation in the SMILE extends standard model evaluation, which is mostly based on static statistics. We provide the first comprehensive analysis on heatwave tracks considering internal climate variability conducted within a SMILE, promoting the latter as a methodological testbed in climate extremes research.

1. Introduction

Due to their frequent and often persisting occurrences in extended European regions, heatwaves accounted for substantial economic, social, health, and ecologic impacts and loss during the past years.

Local heatwave occurrence is commonly associated with various dynamic or thermodynamic drivers. Dynamic drivers include anticyclonic, sometimes quasi-stationary ('blocking') conditions fostering local heating during subsidence processes or heat advection (Lhotka *et al* 2018, Simmonds 2018, Shafiei Shiva *et al* 2019, Li *et al* 2020, Suarez-Gutierrez *et al* 2020). Blocking is known to be connected to Northern Hemisphere temperature extremes (see also Zhuo *et al* 2022). Thermodynamic drivers refer to soil moisture conditions affecting evaporative cooling (Hirschi *et al* 2011, Jaeger and Seneviratne 2011) or local

and upwind land-atmosphere coupling (Fischer *et al* 2007, Lhotka and Kyselý 2015b, Schumacher *et al* 2019) which may both be influenced by preceding seasonal precipitation deficits (Della-Marta *et al* 2007, Vautard *et al* 2007, Bastos *et al* 2020, Felsche *et al* 2022). Associated to the latter, anthropogenic land use changes like albedo effects, humidity and radiation budget changes due to imperviousness alteration, i.e. urbanization, regionally explain considerable portions of heatwave variability (Li *et al* 2021, Wu *et al* 2021). Studies show that favorable projected changes in these drivers or their combinations imply increases in heatwave number, duration, and intensity under changing climate conditions which stresses the importance of quantifying heatwave characteristics (Meehl and Tebaldi 2004, Shafiei Shiva *et al* 2019, Molina *et al* 2020, Suarez-Gutierrez *et al* 2020) for adaptation.

Additionally, scientific knowledge on geographical heatwave characteristics is key to adaptation, be it the derivation of distinct geographical heatwave regions in Europe by means of clustering (Stefanon *et al* 2012), the integration of spatio-temporal characteristics in a heat severity index (Keellings and Moradkhani 2020), inter-model differences of typical spatial patterns (Gibson *et al* 2017, Molina *et al* 2020), or ranking of historical events regarding their extent and intensity (Russo *et al* 2015, Lhotka and Kyselý 2015a, 2015b). Depending on the size and shape of regions affected by heatwaves, people exposure and energy demand for cooling may increase, especially in regions not acclimatized to high temperatures (Smith *et al* 2013, Lyon *et al* 2019). While the spatial extent of heatwaves is captured by temporally aggregated measures like the *heatwave magnitude index daily* (HWMId, Russo *et al* 2015), they miss the temporal evolution of heatwaves.

Increased knowledge on the spatio-temporal evolution of heatwaves offers the opportunity for warning and preparation along their propagation pathways (Clemesha *et al* 2018, Lo *et al* 2021). Thus, not only defining static heatwave regions, but also considering their time-dependent positions is crucial in heatwave prediction (Clemesha *et al* 2018), analysis (Sánchez-Benítez *et al* 2020, Lo *et al* 2021), or impact assessment. For example, Stefanon *et al* (2012) present the temporal sequence of spatial European heatwave clusters, but without further investigating potentially preferential sequences. Clemesha *et al* (2018) investigate the propagation and characteristics of observed California heatwaves when passing pairs of distinct geographical regions. Others follow a Lagrangian perspective by determining major heating processes within European heatwave trajectories (Bieli *et al* 2015, Zschenderlein *et al* 2019), or by tracking global drought displacement (Herrera-Estrada *et al* 2017, Herrera-Estrada and Diffenbaugh 2020). Spensberger *et al* (2020) find that one observed transition among heatwaves in distant regions, Central European–Scandinavian successions in 2003 and 2018, occurred coincidentally based on dynamics investigations.

These analyses do not generalize heatwave track characteristics and fail to explain the reasons of specific tracks. Thus an approach to (a) derive typical heatwave tracks, and (b) summarize track specifics is needed, in order to (c) associate tracks with explanatory variables. We attempt to extend and generalize the idea of establishing dynamical links among heatwaves occurring in close temporal and spatial vicinity.

An elegant solution to derive directed links among spatio-temporal phenomena, including the information on link significance, effect size, and temporal lags of signal propagation, is provided by causal discovery algorithms. Causal discovery or causal inference allows harvesting the potential of climate big data to gain knowledge on processes by deriving

hypotheses on causal interdependence hidden in (observational) data (Ebert-Uphoff and Deng 2012a, Deng and Ebert-Uphoff 2014, Runge *et al* 2019a, 2019b). More specifically, Runge *et al* (2019b) mention causal hypothesis testing, climate network analysis, driver identification with respect to extreme impacts or model evaluation as potential applications in climate research. So far, causal discovery was used to obtain networks of information flow within the atmosphere, e.g. portraying westerly atmospheric flows (Ebert-Uphoff and Deng 2012b), or the identification of major atmospheric perturbation ‘gateways’ related to teleconnections (Runge *et al* 2015). Almendra-Martín *et al* (2022) use a causal discovery algorithm to identify the influence of climate modes on soil moisture variability. Very recently, first climate model ensemble based investigations of teleconnections were performed (Galytska *et al* 2022, Karmouche *et al* 2022).

Transferring the concept of information flow (Runge *et al* 2015) to the heatwave propagation question, we suggest interpreting heatwave movements as temporally lagged heatwave onset in distinct regions. We propose a generalized approach to explain heatwave propagation based on causal discovery and examine potential explanations for derived pathways. This study builds on results from a previous study (Felsche *et al* 2022), where recurrent heatwave core regions were derived by means of clustering. We hypothesize that distinct recurring propagation tracks can be identified beyond single events in Europe. To generalize from observed event sequences we employ a single-model initial condition large ensemble (SMILE) of a regional climate model. This increases the sample of potential heatwave tracks and allows to evaluate observed tracks with respect to naturally occurring climate variability in high spatio-temporal resolution.

2. Methodology

Our approach to track heatwaves consists of four steps: (a) define each day within the analysis period meeting preset criteria as a heatwave (hot day), (b) cluster all hot days with respect to their geographical extent into core regions, (c) aggregate these core regions into time series and (d) apply a causal discovery algorithm to derive directed links among the core region time series.

2.1. Data and validation

Observational records provide a limited amount of heatwave events in Europe. Thus, employing a SMILE allows to increase the sample size: By using the Canadian Regional Climate Model, version 5, Large Ensemble (CRCM5-LE, Leduc *et al* 2019) we obtain 50 members of comparable climate statistics to derive robust results at high spatial resolution (0.11°, 12.5 km) while considering internal climate

variability. While the CRCM5-LE was already extensively used for analyses on rare (hydrometeorological) extremes (Champagne *et al* 2020, Wood and Ludwig 2020, Böhnisch *et al* 2021, Brunner *et al* 2021, Poschlod and Ludwig 2021), the present study is the first to apply causal inference where large samples are also of importance (Spirtes and Glymour 1991, Runge *et al* 2019b).

We pool the period 1981–2010 from 50 members into one 1500 year time series. Since all members are designed to share comparable climate statistics, typical patterns and subsequently pathways of phenomena are assumed to be comparable across all members (and to reality), only varying due to internal climate variability (Leduc *et al* 2019).

For heatwave definition, we use daily maximum temperature (tasmax). Daily 500 hPa geopotential height (Z500) is employed for large-scale atmospheric pattern definition. We first perform heatwave clustering and track derivation on a ERA-Interim driven (Dee *et al* 2011) run of CRCM5 (CRCM5/ERA, Leduc *et al* 2019) in order to evaluate them against historical events while using the same regional climate model. Additionally, an external evaluation on the E-OBS gridded dataset (version 22.0e at 0.1° spatial resolution; Haylock *et al* 2008, Cornes *et al* 2018) is performed (figure S1). All analyses are confined to land areas within a European domain (Leduc *et al* 2019).

2.2. Heatwave definition

Heatwave definitions in literature vary according to study perspectives (Perkins and Alexander 2013, Smith *et al* 2013, Shafiei Shiva *et al* 2019). To properly assess heatwave tracks, our heatwave definition requires information for each time step (day) under consideration. We define heatwaves relative to local climatology (Della-Marta *et al* 2007) as a minimum of three consecutive hot days, separated by at least three non-hot days (Keellings and Moradkhani 2020, Spensberger *et al* 2020) from the preceding/following hot day: a hot day occurs if the centered three-day-running mean of tasmax exceeds the local 95th JJA (1981–2010) percentile (similar to Lhotka and Kyselý 2015a). Negative anomalies are omitted. Whereas the percentile in a single run or observation/reanalysis may be poorly estimated due to the limited sample size (30 years), uncertainty due to internal variability is reduced in the SMILE by deriving the percentile from a 1500 year sample. Additionally, percentile based anomalies reduce potential inconsistencies among the data sources induced by climate model bias.

Spurious artifacts ($\leq 9 \times 9$ pixels) and isolated hot day occurrences are removed. A time step is considered as belonging to an extended heatwave event, if hot days occur in at least 1% of the land area in the domain (i.e. 500 grid cells). All matching time steps are next used to derive core regions by clustering (Felsche *et al* 2022). Preliminary analyses revealed hot

days in months May–October, such that we splice this period over all years and members (Ebert-Uphoff and Deng 2012a).

2.3. Location of core regions

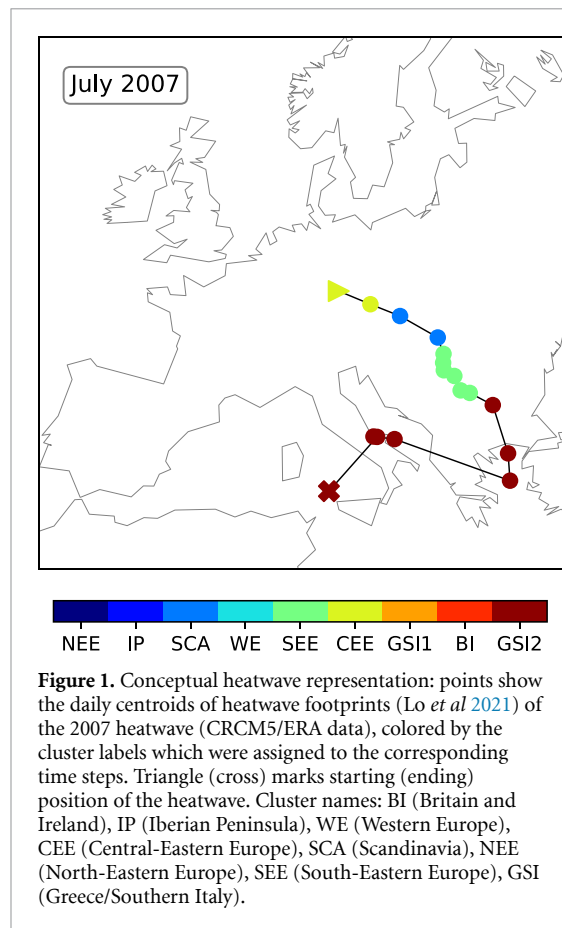
For core region definition, we refer to spatially coherent recurring patterns of European heatwaves by means of clustering (Felsche *et al* 2022).

Clustering is frequently employed for mid-latitude weather pattern analysis and classification (Smyth *et al* 1997, Stefanon *et al* 2012, Lhotka and Kyselý 2015a, Hannachi *et al* 2017, Wang *et al* 2018, Keellings and Moradkhani 2020, Machado and Lopes 2020). We use daily maps of hot day occurrences as input to a two-step agglomerative hierarchical clustering (Felsche *et al* 2022). The optimal number of clusters is determined by computing the distortion score for every possible number of clusters and piking the knee of the curve (Jung *et al* 2003). When comparing cross-validation clustering results against cluster results from a Monte-Carlo pseudo-experiment, nine spatial heatwave patterns are obtained which are significant on the 99% level based on a two-sided t-test (Felsche *et al* 2022). These cluster footprints correspond well with historical events captured by other heatwave indexes (e.g. Russo *et al* 2015). Felsche *et al* (2022) shows high consistency among clusters in CRCM5/ERA and CRCM5-LE. We follow their naming conventions for CRCM5-LE: BI (Britain and Ireland), IP (Iberian Peninsula), WE (Western Europe), CEE (Central-Eastern Europe), SCA (Scandinavia), NEE (North-Eastern Europe), SEE (South-Eastern Europe), GSI (Greece/Southern Italy). Sequences of time steps labeled according to their respective clusters then represent single heatwaves (figure 1).

Next, clustered time steps are spatially averaged, using the normalized intensity of temporally averaged cluster footprints as weights for their centroid coordinates (Herrera-Estrada *et al* 2017, Herrera-Estrada and Diffenbaugh 2020, Sánchez-Benítez *et al* 2020). This provides nine time series of positive temperature anomalies, located at the cluster footprint centers (i.e. their centroids) and representing the components (Runge *et al* 2015) among which spatio-temporal links are to be established. A sensitivity experiment using different weights for aggregation and therefore time series positioning revealed no major changes in link directions. Since CRCM5/ERA and CRCM5-LE provide slightly different cluster footprints, the positions of these time series diverge as well (see figure 2(a) and figure S1 for E-OBS).

2.4. Transitions among core regions by means of causal discovery

In order to analyze heatwave tracks between heatwave onset and offset, we split them into transitions among core regions. This captures direct movements between various regions. Location changes within



cluster regions or growth and shrinkage of the spatial extent without heatwave core shifts are considered as stationary.

A heatwave moves from region A to region B, if heatwave onset in region A is followed by heatwave onset in region B, and if heatwave onset in region B was preceded by heatwave onset in region A: The heatwave stays in region A until day t and moves to region B at day $t+1$. We thus aim to explain a later position of a heatwave by its previous position (i.e. effect preceded by its cause).

Generally in causal discovery, distinct nodes representing single processes (variables or locations of the same variable) are derived prior to link establishing, by e.g. sampling of equally spaced grid points or rotated principal component analysis (Ebert-Uphoff and Deng 2012b, Deng and Ebert-Uphoff 2014, Runge *et al* 2015, 2019a, Nowack *et al* 2020). Here, we employ time series assigned to nine spatially distributed clusters of heatwave core regions.

To define linear spatio-temporal links among heatwave core regions we employ a causal discovery algorithm provided with the *Tigramite 5.1* Python package, namely the PCMCI algorithm (Runge *et al* 2019a, Nowack *et al* 2020). It is based on the PC algorithm introduced by Spirtes and Glymour (1991): First, a fully connected graph of all variables (nodes) under consideration, e.g. time series at different locations, is created. Then, conditionally independent

links (edges) are deleted, while for the remaining links directions are identified (e.g. by considering a temporal ordering of cause and effect) (Ebert-Uphoff and Deng 2012a, Deng and Ebert-Uphoff 2014, Runge *et al* 2019b). An amelioration with respect to time series is provided by the two-step PCMCI algorithm, adding a momentary conditional independence test to the PC algorithm (Runge *et al* 2019a, Nowack *et al* 2020): it rejects spurious or indirect links by testing for independence conditional on the common past of network nodes. Thus, only direct links among network nodes are kept which goes beyond pure pairwise correlation graphs (Runge *et al* 2019b). The PCMCI algorithm can be more powerful than correlation analysis in determining relationships between variables, even in finding links which may not be obvious in classic correlation analysis (Almendra-Martín *et al* 2022). Additionally, it bears the potential to find indirect links and consider common drivers as opposed to other forms of causal discovery like Granger causality (Granger 1969, Runge *et al* 2019b, Galytska *et al* 2022).

In this present study, conditional independence tests are conducted based on partial linear correlations (ParCorr) with a significance threshold of $\alpha = 10^{-3}$. We use a minimum temporal lag of one day, reflecting transitions, and a maximum of three days, reflecting the three days separating two heatwaves. Additionally, we focus on positively correlated links because negative correlations would correspond to the non-occurrence of heatwaves in region B after occurrence in region A.

2.5. Explaining heatwave tracks

The importance of heatwave drivers varies regionally (Zschenderlein *et al* 2019), with dynamical mechanisms generally dominating over local thermodynamical ones (Suarez-Gutierrez *et al* 2020). As mentioned previously, high pressure, i.e. positive Z500 height anomalies, may lead to subsidence, cloud dispersal and subsequently enhanced heating at the surface. Additionally, prevailing dry conditions, e.g. low soil moisture contents, amplify the heating process by reducing the latent heat flux. Both drivers may interact and intensify, e.g. in feedback loops (Fischer *et al* 2007), since prevailing heat in turn may increase evaporation, thereby leading to further soil drying (Schumacher *et al* 2019).

We focus on associated large-scale Z500 conditions to investigate why heatwaves follow a given track. Patterns similar to the Z500 anomaly composites alongside selected heatwave transitions are searched during months May–October. Thereupon we calculate the probabilities of (a) having this pattern during an eight-day period centered at the indicated transition and (b) of having this transition during the indicated pattern. Pattern similarity is assessed by means of masking: if at least 66% of grid cells at an arbitrary time step show positive anomalies inside the

composite positive anomaly region, and if at the same time an analogous agreement is achieved within the composite negative anomaly region, this time step is considered as being similar to the composite pattern. Consecutive days of similar patterns are summarized as one occurrence, which is related to atmospheric circulation persistence (see Jézéquel *et al* 2018, who relate atmospheric patterns to hot days by means of Euclidean distance calculation).

3. Results

3.1. Spatial propagation of heatwaves

During 1981–2010, 115 European heatwaves with at least three days are identified in CRCM5/ERA compared to 5425 in the 50-member CRCM5-LE. Most heatwaves occur during summer months JJA, starting earlier in the West than in the East (Felsche *et al* 2022). The relative frequency of heatwaves ending in the Eastern parts of Europe is increased compared to the frequency of heatwaves starting there (figure 2(a)). Accordingly, heatwaves start more frequently in the Western parts of Europe. Taken together, these first findings indicate a general west-to-east movement of heatwaves in both CRCM5/ERA and CRCM5-LE, which mirrors the dominating westerly flow onto Europe (e.g. Zschenderlein *et al* 2019). Heatwaves starting outside the defined core regions, e.g. outside the domain, over Northern Africa or the ocean, are not captured.

Most heatwaves consist of several transitions (figures 2(b) and (c)). While in general the number of transitions increases with heatwave length, very stationary heatwaves extend up to 20 days within one cluster and highly mobile heatwaves encounter 6 transitions in ten days. CRCM5-LE shows a stronger variability among transition–length combinations than CRCM5/ERA, representing natural variability of heatwave characteristics. The three historical examples 2003, 2006, and 2010 exhibit extreme lengths with respect to the majority of events (e.g. three transitions in 44 days in 2010).

A more detailed network of statistical robust sequences among neighboring core regions is provided in figures 3(a) and (b). It represents a mixture of latitudinal and longitudinal transition directions like a spine of the continental landmasses: While in the West, a South-Northward direction prevails, the East experiences the opposite direction. Within the scope of our study, we focus on links with lag = 1 among two core regions at a time. In order to obtain robust results, links were first derived on the entire 1500-summer period. To include internal variability of these, they were also calculated for each member separately, allowing to count their frequency. In figure 3, only links occurring in at least 15 members (i.e. 30% of the ensemble) are presented with colors indicating their frequency (compare Galytska *et al* 2022, Karmouche *et al* 2022, for alternative

presentation methods in ensembles). As a real-world example, the July 2007 heatwave (figure 1) is represented within the SEE–GSI link.

In order to further evaluate the obtained links, we next compare the graph based on model data with reanalysis and observation based links (compare Karmouche *et al* 2022). While most of these links figure in the CRCM5/ERA and E-OBS network as well (figures S1(a) and (c)), several links from historical data are missing within the robust CRCM5-LE links, being thus (most likely) rare outliers. Others are shifted compared to CRCM5-LE since the position of core regions diverges. The CRCM5-LE links show higher correspondence to the representation in CRCM5/ERA (F1-scores among members and reference above 0.5, figure S2) than to the one in E-OBS (F1-scores close to 0.2; most likely due to clearly shifted or split core regions like, e.g. GSI). Additionally, no link connecting CEE and SCA can be established in CRCM5/ERA as was also found in Spensberger *et al* 2020. Since CRCM5-LE shows these links in 16 and 30 members, respectively, it is likely not observed in CRCM5/ERA due to potential errors in reference causal graph reconstruction (Galytska *et al* 2022) or internal variability. Exact agreement between reference data and model network cannot be expected due to internal climate variability. However, larger ensemble sizes increase the likelihood of capturing observed relationships within the ensemble range (compare Karmouche *et al* 2022).

Due to algorithm construction, the absence of links is a more robust result than their existence: if no statistical link can be established among two nodes, it is unlikely that a physical process links both under the assumption of data faithfully representing the underlying physical processes (Runge *et al* 2019a). All links are highly invariant towards leaving out arbitrary nodes in calculation (except for nodes contained in a given link, figure 3(b)).

We next analyze pairs of core regions before and after transitions, i.e. the links derived in figure 3. All selected transitions occur most often during July and August (figure 4(a)); however, transitions in Western and North-Western regions tend to occur earlier (beginning of July) than South-Eastern regions (beginning of August) with the exception of transition IP–WE2. This is connected to the seasonal preference of heatwave clusters themselves (Felsche *et al* 2022).

The links found in figure 3 are next evaluated against all possible links between the first and second cluster in a transition (k_1 and k_2). All of them rank among the top three most frequent transitions from their respective starting cluster (figures 4(b) and (c)). Transition occurrences of IP–WE2, WE2–BI and SEE–GSI, i.e. comparably short distances, exceed the expected value of randomly occurring transitions (i.e. k_1 and k_2 being independent) by factor 3 or 4. Among these, SEE–GSI mirrors source region–target region

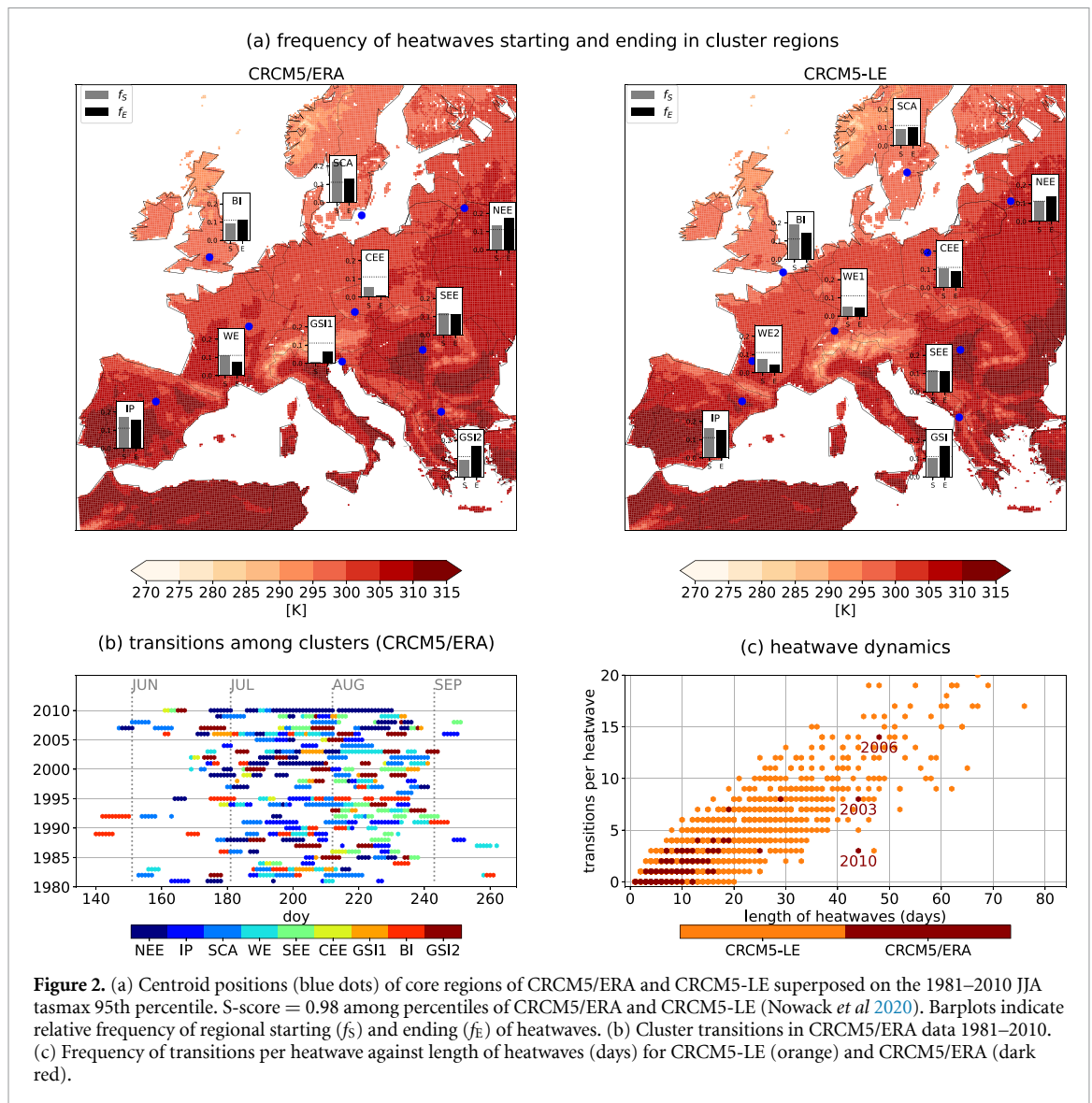


Figure 2. (a) Centroid positions (blue dots) of core regions of CRCM5/ERA and CRCM5-LE superposed on the 1981–2010 JJA tasmax 95th percentile. S-score = 0.98 among percentiles of CRCM5/ERA and CRCM5-LE (Nowack *et al* 2020). Barplots indicate relative frequency of regional starting (f_s) and ending (f_e) of heatwaves. (b) Cluster transitions in CRCM5/ERA data 1981–2010. (c) Frequency of transitions per heatwave against length of heatwaves (days) for CRCM5-LE (orange) and CRCM5/ERA (dark red).

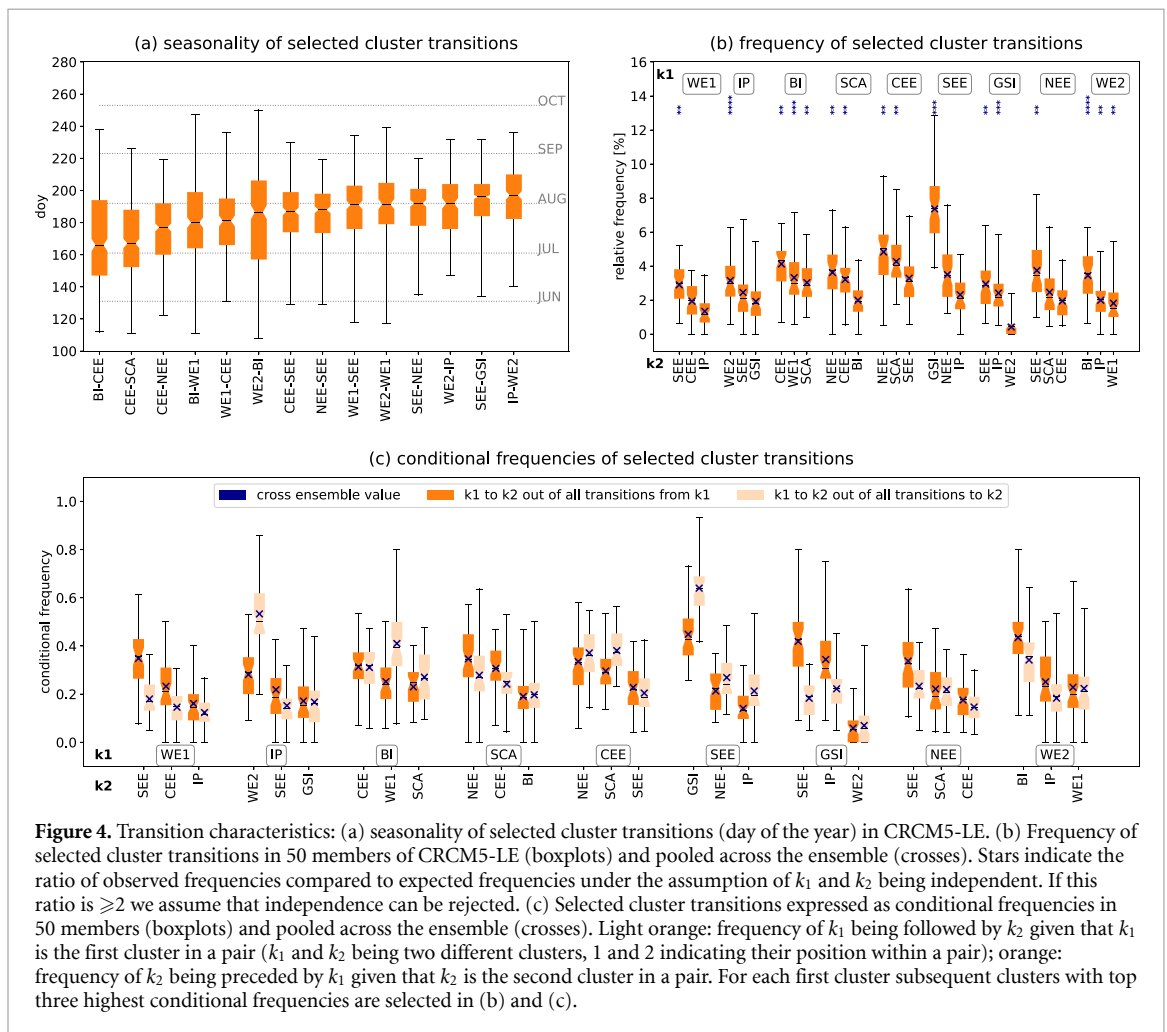
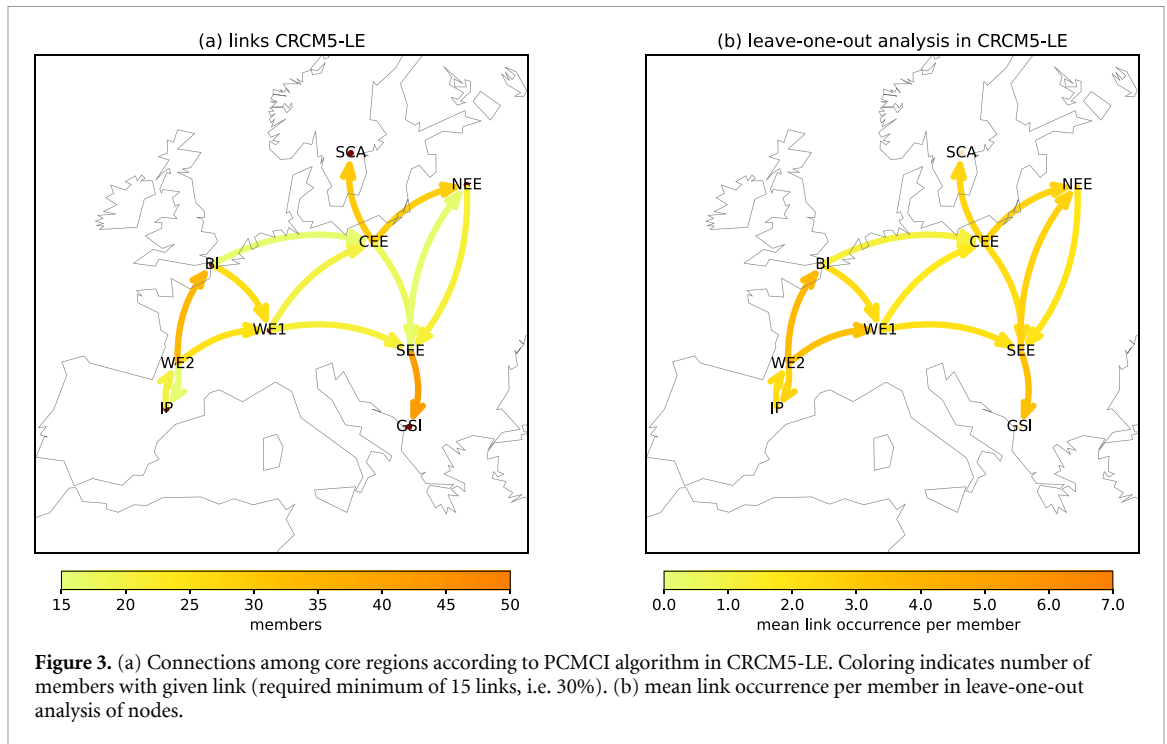
directions of trajectories found in Bieli *et al* 2015. The authors also identify trajectory source regions for heatwaves in the BI region west to Great Britain, which is not represented in figure 3. Generally, source regions (i.e. start regions in our analysis) of air masses are located close to heatwave occurrence regions (Bieli *et al* 2015).

Expressing transition strength in terms of conditional frequencies, figure 4(c) supports the results from the causal discovery network: Values of 1 would indicate a strict connection between both clusters, i.e. k_1 is always followed by k_2 and k_2 being always preceded by k_1 . In other words, heatwave occurrence in k_1 is likely a sufficient and necessary condition for heatwave occurrence in k_2 . Figure 4(c) shows high cross-ensemble values (and thus suggests strong connections) for, e.g. transitions SEE–GSI or IP–WE2, but also large variability among members: In 45% of all SEE occurrences, the heatwave propagates to GSI. Equally close connections characterize transitions WE2–BI (43%) or GSI–SEE

(42%). This indicates a preference of heatwaves moving from the given first core region to the corresponding second core region within the analysis period.

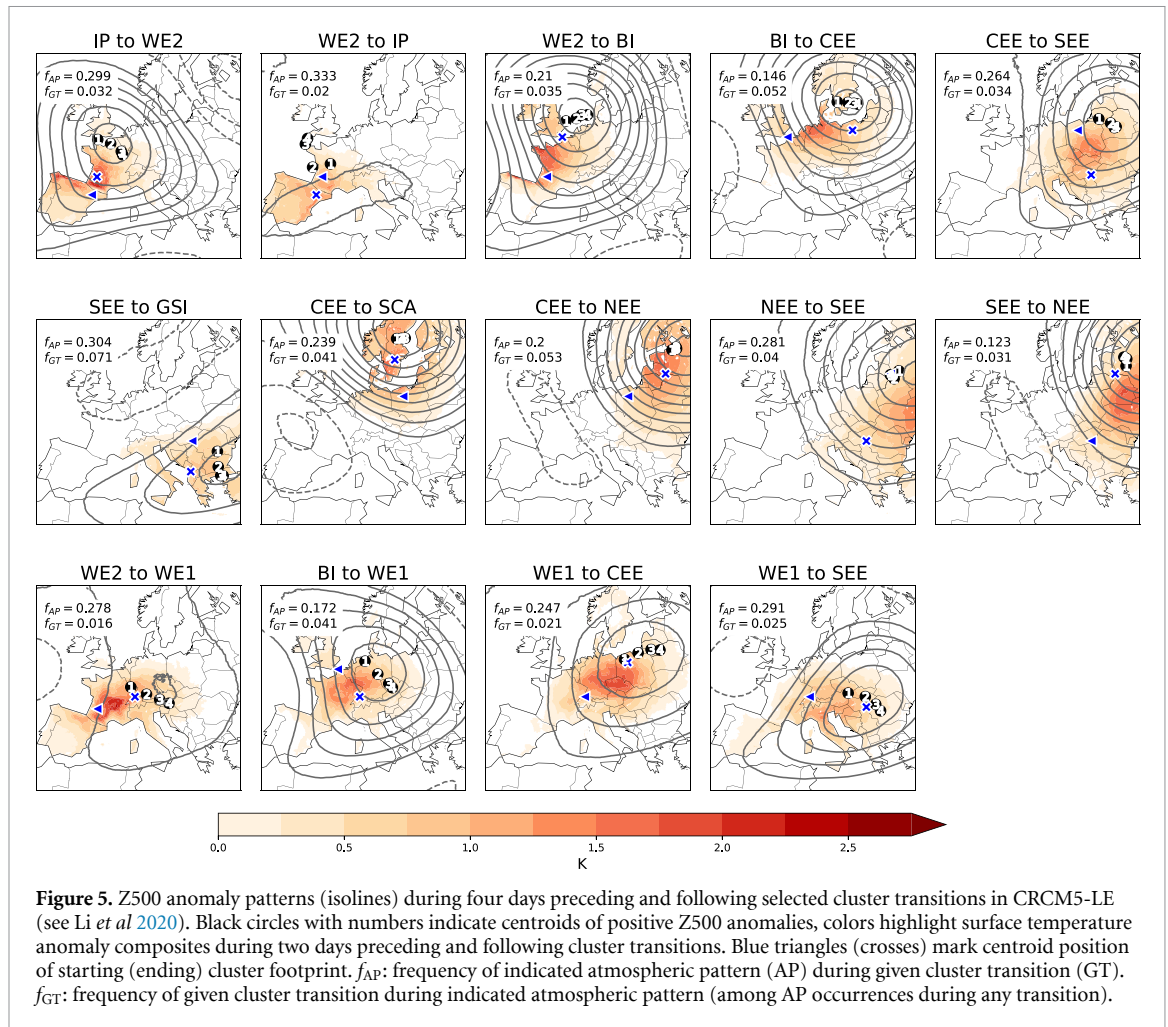
3.2. Associated dynamic conditions

We next seek to connect these previously discussed transitions with potential drivers explaining their pathways (figure 5). Since negative soil moisture anomalies prevail before and after the transitions in the core regions (figure S3), we focus on centroid positions of positive Z500 anomalies during the two days preceding and two days following an indicated transition (figure 5). Our hypothesis states that a moving center of high pressure anomalies, as strong predictors of heat (Suarez-Gutierrez *et al* 2020), draws heatwaves with it in a similar direction. Acknowledging the fact that single events may deviate from these composites and the link between composites and heatwave occurrence may be not specific (Boschat *et al* 2016,



Clemesha et al 2018, Zschenderlein et al 2019), we only examine regions where the signal exceeds the standard error among composite components. As was

found for stationary heatwave patterns (Stefanon et al 2012), Z500 anomaly composites and temperature patterns correspond well in their spatial extent during



transitions. Some heatwave footprints, however, are observed to be larger than their associated synoptic patterns (Spensberger *et al* 2020). The IP–WE2 Z500 and heat anomaly patterns as well as the propagation tracks are similar to the ‘European Cluster’ in Sánchez-Benítez *et al* 2020.

In general, Z500 anomalies are located to the North-East of the heatwave core regions (compare crosses and triangles in figure 5). Blocking is known to intensify hot extremes southwest of its occurrence by various heating processes and advecting warm continental air masses (Pfahl 2014). For BI–CEE, CEE–SEE, BI–WE1, WE1–SEE, and SEE–GSI, centroid positions of Z500 anomalies lie between start and end positions of the transitions, in parts clearly mirroring the movement direction (see positions of 1–4 relative to each other, figure 5, and figure S3 for a comparison of selected links with CRCM5/ERA).

These associated patterns tend to appear during 12%–33% of the respective transitions in CRCM5-LE. Unsurprisingly, relative occurrences of the indicated transitions during all pattern occurrences remain low (0.1%–0.8%), given a high frequency of these patterns during May–October. Thus, the specific Z500 pattern occurrence is very likely not a sufficient cause for transition occurrence, but may be treated

as a necessary condition (see Boschat *et al* 2016, Hannart *et al* 2016). Among pattern occurrence during any heatwave transition, however, the indicated transitions occur up to ten times more frequently, ranging from 2% to 7%. To summarize, associated pattern occurrence alone cannot be interpreted as a clear sufficient or necessary condition to causally explain heatwave transitions, although they tend to propagate in the same direction as contemporaneous heatwaves.

4. Discussion

By employing a framework involving causal discovery, we find indications of distinct heatwave tracks in Europe during 1981–2010. A very recent example of their meaningfulness is the July 2022 heatwave in Europe which started on the Iberian Peninsula, propagated towards Western Europe, Great Britain, Central-Eastern Europe and last to South-Eastern Europe (ECMWF 2022).

In parts, heatwave tracks are explained by large-scale circulation patterns (land-atmosphere or sea surface temperature related drivers were outside the study scope). Our approach allows to extract information on heatwave direction, dislocation velocity and

seasonal occurrence along these tracks. These analyses are intended to understand a facet of spatially distributed extreme events, especially heatwaves, but not specifically to add to local prediction. Defining core regions based on naturally occurring geographical patterns of heatwaves rather than analyzing at arbitrarily chosen coordinates allows to perform a meaningful complexity reduction by grouping coherent spatial patterns to one core region. Causal discovery facilitates the comprehensive connection of heatwave regions across space and time and thus merges two dimensions which are commonly investigated separately. Moreover, it isolates dominant heatwave directional movements from a large dataset and identifies target regions of heatwave tracks.

Further investigation of recurrent heatwave tracks regarding the spatially varying interplay (Suarez-Gutierrez *et al* 2020) and importance of their respective drivers (as e.g. in Wu *et al* 2021) bears the potential to improve heatwave prediction or attenuation of regional driving factors by e.g. suitable land cover changes (Miralles *et al* 2019).

There are some limitations to our approach. First, employing a causal discovery algorithm requires certain conditions to be met (Spirtes and Glymour 1991, Ebert-Uphoff and Deng 2012a, Runge *et al* 2015): In order to correctly derive a network of directed links, all variables of relevance need to be included in the analysis (causal sufficiency). A spatially constrained domain may exclude regions of concern to the phenomenon. We attempt to evade this problem by constraining our analysis to land masses of Europe, i.e. heatwaves starting and ending in Europe. Moreover, large scale air mass flow—as shown to be related to heatwave tracks—dominantly follows a west-east path in Europe, thus leaving our domain towards the cut-off side. In order to clarify the influence of potentially missing nodes or variables outside the domain, we performed a leave-one-out analysis mimicking different ‘domain sizes’. The analysis showed no considerable changes to the network (figure 3(b)). Thus, even if pathways entering/exiting the domain were missing, links within the domain would remain widely undisturbed. Consequently, the obtained links are valid with respect to the included nodes only as is also mentioned in Karmouche *et al* 2022.

This leads to the question why using a regional domain and not a global one, which may have avoided this problem. However, the selection of a small spatial domain reduced the risk of having several heatwaves with no common origin at the same time. Moreover, using a spatial resolution of 0.11° as opposed to, e.g. 1° or 2.8° , leads to higher precision of spatial pattern delineation in heterogeneous landscapes (Molina *et al* 2020) and thus improves core region location.

Using a SMILE allows to derive a large variety of events and, consequently, of transitions among regions. This offers the opportunity to investigate

likelihoods of links: For example, WE2–BI, SEE–GSI and CEE–NEE are more robust against the backdrop of internal variability than BI–CEE, CEE–SEE or NEE–SEE. Furthermore, in single realizations of reanalysis/observations long-lasting heatwaves may bias the clustering towards these events. For example, during the persistent 2010 heatwave in Russia, two clusters dominate (figure 2(b)), whereas clustering among 1500 rather than 30 years increases the likelihood of having various different spatial heatwave patterns as a baseline. Additionally, since heatwave tracks are extremely dependent on the exact weather patterns, small samples may bias expectations for larger samples. This was also found when investigating causal discovery links of single SMILE members (e.g. regarding CEE–SCA). Possibly large multi-model uncertainties (Nowack *et al* 2020) are beyond the scope of this study, but should be further investigated, e.g. in SMILEs of different models.

5. Summary and conclusions

In this study, we not only use causal discovery to derive observed spatio-temporal propagation of a phenomenon, but also to investigate spatio-temporal extremes on a more general ground for the first time in a SMILE. Thus the SMILE serves as a methodological testbed to investigate the power of causal discovery in abstracting spatio-temporal links from single event analyses. Additionally, we are able to infer that spatio-temporal links are represented plausibly in our SMILE which adds to common model evaluation based on static statistical metrics.

Causality in this study is understood as explaining the occurrence of heat anomalies at a given location by occurrences at more distant locations. Similar to established methods of heatwave tracking, our method is not confined to this type of spatial extremes and may be extended to investigate dominating land-fall heatwave/drought paths.

We suggest that as high pressure anomalies propagate across Europe, associated high temperatures move along. Surface-atmospheric processes, e.g. moisture availability, evaporation, or heating of dry landscapes, may enhance or reduce temperatures, leading to a decoupling of Z500 and temperature anomalies after some time. A more detailed analysis of heat origins or temperature evolution during heatwaves (e.g. associated to Z500 timeseries) may extend the understanding of heatwave propagation. Further studies could also include investigations as to how heatwaves tracks and their connection to large-scale atmospheric patterns evolve under changing climate conditions or in different seasons. In order to verify model representation of heatwave tracks, we propose to repeat similar analyses in further (high-resolution) SMILEs. This could also help to better estimate the influence of domain choice.

If communicated broadly, recurring connections among core regions may foster awareness among people living in a downstream region whenever an upstream region is already affected by a heatwave.

Data availability statement

The data that support the findings of this study are available upon reasonable request from the authors.

Acknowledgments

This research was conducted within the ClimEx project (www.climex-project.org) funded by the Bavarian State Ministry for the Environment and Consumer Protection (Grant No. 81-0270-024570/2015). CRCM5 was developed by the ESCER Centre of Université du Québec à Montréal (UQAM; <https://escer.uqam.ca/>, last access: 16 August 2022) in collaboration with Environment and Climate Change Canada. The authors gratefully acknowledge the Leibniz Supercomputing center for funding this project by providing computing time on its Linux-Cluster. The authors would like to thank M Mittermeier, L Suarez Gutierrez and R Wood for discussions. The *tigramite* algorithm is provided via GitHub by J Runge.

ORCID iD

A Böhnisch  <https://orcid.org/0000-0001-7496-1478>

References

- Almendra-Martín L, Martínez-Fernández J, Piles M, González-Zamora A, Benito-Verdugo P and Gaona J 2022 Influence of atmospheric patterns on soil moisture dynamics in Europe *Sci. Total Environ.* **846** 157537
- Bastos A et al 2020 Direct and seasonal legacy effects of the 2018 heat wave and drought on European ecosystem productivity *Sci. Adv.* **6** eaba2724
- Bieli M, Pfahl S and Wernli H 2015 A lagrangian investigation of hot and cold temperature extremes in Europe *Q. J. R. Meteorol. Soc.* **141** 98–108
- Böhnisch A, Mittermeier M, Leduc M and Ludwig R 2021 Hot spots and climate trends of meteorological droughts in Europe—assessing the percent of normal index in a single-model initial-condition large ensemble *Front. Water* **3** 716621
- Boschat G, Simmonds I, Purich A, Cowan T and Pezza A B 2016 On the use of composite analyses to form physical hypotheses: An example from heat wave—SST associations *Sci. Rep.* **6** 29599
- Brunner M I, Swain D L, Wood R R, Willkofer F, Done J M, Gilleland E and Ludwig R 2021 An extremeness threshold determines the regional response of floods to changes in rainfall extremes *Commun. Earth Environ.* **2** 173
- Champagne O, Leduc M, Coulibaly P and Arain M A 2020 Winter hydrometeorological extreme events modulated by large-scale atmospheric circulation in southern ontario *Earth Syst. Dyn.* **11** 301–18
- Clemesha R E S, Guirguis K, Gershunov A, Small I J and Tardy A 2018 California heat waves: their spatial evolution, variation and coastal modulation by low clouds *Clim. Dyn.* **50** 4285–301
- Cornes R C, van der Schrier G, van den Besselaar E J M and Jones P D 2018 An ensemble version of the e-obs temperature and precipitation data sets *J. Geophys. Res.: Atmos.* **123** 9391–409
- Dee D P et al 2011 The era-interim reanalysis: configuration and performance of the data assimilation system *Q. J. R. Meteorol. Soc.* **137** 553–97
- Della-Marta P M, Luterbacher J, von Weissenfluh H, Xoplaki E, Brunet M and Wanner H 2007 Summer heat waves over western Europe 1880–2003, their relationship to large-scale forcings and predictability *Clim. Dyn.* **29** 251–75
- Deng Y and Ebert-Uphoff I 2014 Weakening of atmospheric information flow in a warming climate in the community climate system model *Geophys. Res. Lett.* **41** 193–200
- Ebert-Uphoff I and Deng Y 2012b A new type of climate network based on probabilistic graphical models: Results of boreal winter versus summer *Geophys. Res. Lett.* **39** L19701
- Ebert-Uphoff I and Deng Y 2012 Causal discovery for climate research using graphical models *J. Clim.* **25** 5648–65
- ECMWF 2022 Update on European heatwave of July 2022 (available at: www.ecmwf.int/en/about/media-centre/focus/2022/update-european-heatwave-july-2022) (Accessed 22 July 2022)
- Felsche E, Böhnisch A and Ludwig R 2022 Inter-seasonal connection of typical European heatwave patterns to soil moisture Research Square pp 1–25 (<https://doi.org/10.21203/rs.3.rs-1673999/v1>)
- Fischer E M, Seneviratne S I, Lüthi D and Schär C 2007 Contribution of land-atmosphere coupling to recent European summer heat waves *Geophys. Res. Lett.* **34** L06707
- Galytska E, Weigel K, Handorf D, Jaiser R, Köhler R H, Runge J and Eyring V 2022 Causal model evaluation of arctic-midlatitude teleconnections in cmip6 *Earth Space Sci. Arch.* **1**–33
- Gibson P B, Perkins-Kirkpatrick S E, Alexander L V and Fischer E M 2017 Comparing australian heat waves in the cmip5 models through cluster analysis *J. Geophys. Res.: Atmos.* **122** 3266–81
- Granger C W J 1969 Investigating causal relations by econometric models and cross-spectral methods *Econometrica* **37** 424–38
- Hannachi A, Straus D M, Franzke C L E, Corti S and Woollings T 2017 Low-frequency nonlinearity and regime behavior in the northern hemisphere extratropical atmosphere *Rev. Geophys.* **55** 199–234
- Hannart A, Pearl J, Otto F E L, Naveau P and Ghil M 2016 Causal counterfactual theory for the attribution of weather and climate-related events *Bull. Am. Meteorol. Soc.* **97** 99–110
- Haylock M R, Hofstra N, Klein Tank A M G, Klok E J, Jones P D and New M 2008 A European daily high-resolution gridded data set of surface temperature and precipitation for 1950–2006 *J. Geophys. Res.: Atmos.* **113** D20119
- Herrera-Estrada J E and Diffenbaugh N S 2020 Landfalling droughts: Global tracking of moisture deficits from the oceans onto land *Water Resour. Res.* **56** e2019WR026877
- Herrera-Estrada J E, Satoh Y and Sheffield J 2017 Spatiotemporal dynamics of global drought *Geophys. Res. Lett.* **44** 2254–63
- Hirschi M, Seneviratne S I, Alexandrov V, Boberg F, Boroneant C, Christensen O B, Formayer H, Orłowsky B and Stepanek P 2011 Observational evidence for soil-moisture impact on hot extremes in southeastern Europe *Nat. Geosci.* **4** 17–21
- Jaeger E B and Seneviratne S I 2011 Impact of soil moisture-atmosphere coupling on European climate extremes and trends in a regional climate model *Clim. Dyn.* **36** 1919–39
- Jézéquel A, Cattiaux J, Naveau P, Radanovics S, Ribes A, Vautard R, Vrac M and Yiou P 2018 Trends of atmospheric circulation during singular hot days in Europe *Environ. Res. Lett.* **13** 054007
- Jung Y, Park H, Du D-Z and Drake B L 2003 A decision criterion for the optimal number of clusters in hierarchical clustering *J. Glob. Opt.* **25** 91–111

- Karmouche S, Galytska E, Runge J, Meehl G A, Phillips A S, Weigel K and Eyring V 2022 Regime-oriented causal model evaluation of atlantic-pacific teleconnections in cmip6 *EGUSphere* **2022** 1–42
- Keellings D and Moradkhani H 2020 Spatiotemporal evolution of heat wave severity and coverage across the united states *Geophys. Res. Lett.* **47** e2020GL087097
- Leduc M et al 2019 The ClimEx project: a 50-member ensemble of climate change projections at 12-km resolution over Europe and northeastern north America with the Canadian regional climate model (CRCM5) *J. Appl. Meteorol. Climatol.* **58** 663–93
- Lhotka O and Kyselý J 2015 Characterizing joint effects of spatial extent, temperature magnitude and duration of heat waves and cold spells over central Europe *Int. J. Climatol.* **35** 1232–44
- Lhotka O and Kyselý J 2015 Spatial and temporal characteristics of heat waves over central Europe in an ensemble of regional climate model simulations *Clim. Dyn.* **45** 2351–66
- Lhotka O, Kyselý J and Plavcová E 2018 Evaluation of major heat waves' mechanisms in EURO-CORDEX RCMs over Central Europe *Clim. Dyn.* **50** 4249–62
- Li M, Yao Y, Simmonds I, Luo D, Zhong L and Chen X 2020 Collaborative impact of the NAO and atmospheric blocking on European heatwaves, with a focus on the hot summer of 2018 *Environ. Res. Lett.* **15** 114003
- Li X, Fan W, Wang L, Luo M, Yao R, Wang S and Wang L 2021 Effect of urban expansion on atmospheric humidity in Beijing-Tianjin-Hebei urban agglomeration *Sci. Total Environ.* **759** 144305
- Lo S-H, Chen C-T, Russo S, Huang W-R and Shih M-F 2021 Tracking heatwave extremes from an event perspective *Weather Clim. Extremes* **34** 100371
- Lyon B, Barnston A G, Coffel E and Horton R M 2019 Projected increase in the spatial extent of contiguous US summer heat waves and associated attributes *Environ. Res. Lett.* **14** 114029
- Machado J and Lopes A M 2020 Rare and extreme events: the case of covid-19 pandemic *Nonlinear Dyn.* **100** 2953–72
- Meehl G A and Tebaldi C 2004 More intense, more frequent and longer lasting heat waves in the 21st century *Science* **305** 994–7
- Miralles D G, Gentile P, Seneviratne S I and Teuling A J 2019 Land-atmospheric feedbacks during droughts and heatwaves: state of the science and current challenges *Ann. New York Acad. Sci.* **1436** 19–35
- Molina M O, Sánchez E and Gutiérrez C 2020 Future heat waves over the mediterranean from an euro-cordex regional climate model ensemble *Sci. Rep.* **10** 8801
- Nowack P, Runge J, Eyring V and Haigh J D 2020 Causal networks for climate model evaluation and constrained projections *Nat. Commun.* **11** 1415
- Perkins S E and Alexander L V 2013 On the measurement of heat waves *J. Clim.* **26** 4500–17
- Pfahl S 2014 Characterising the relationship between weather extremes in Europe and synoptic circulation features *Nat. Hazards Earth Syst. Sci.* **14** 1461–75
- Poschold B and Ludwig R 2021 Internal variability and temperature scaling of future sub-daily rainfall return levels over Europe *Environ. Res. Lett.* **16** 064097
- Runge J et al 2019 Inferring causation from time series in earth system sciences *Nat. Commun.* **10** 2553
- Runge J, Nowack P, Kretschmer M, Flaxman S and Sejdinovic D 2019 Detecting and quantifying causal associations in large nonlinear time series dataset *Sci. Adv.* **5** eaau4996
- Runge J, Petoukhov V, Donges J F, Hlinka J, Jajcay N, Vejmelka M, Hartman D, Marwan N, Paluš M and Kurths J 2015 Identifying causal gateways and mediators in complex spatio-temporal systems *Nat. Commun.* **6** 8502
- Russo S, Sillmann J and Fischer E M 2015 Top ten European heatwaves since 1950 and their occurrence in the coming decades *Environ. Res. Lett.* **10** 124003
- Sánchez-Benítez A, Barriopedro D and García-Herrera R 2020 Tracking Iberian heatwaves from a new perspective *Weather Clim. Extremes* **28** 100238
- Schumacher D L, Keune J, van Heerwaarden C C, Vilà-Guerau de Arellano J, Teuling A J and Miralles D G 2019 Amplification of mega-heatwaves through heat torrents fuelled by upwind drought *Nat. Geosci.* **12** 712–7
- Shafiei Shiva J, Chandler D G and Kunkel K E 2019 Localized changes in heat wave properties across the United States *Earth's Future* **7** 300–19
- Simmonds I 2018 What causes extreme hot days in Europe? *Environ. Res. Lett.* **13** 071001
- Smith T T, Zaitchik B F and Gohlke J M 2013 Heat waves in the United States: definitions, patterns and trends *Clim. Change* **118** 811–25
- Smyth P, Ghil M, Ide K, Roden J and Fraser A 1997 Detecting atmospheric regimes using cross-validated clustering *KDD'97: Proc. 3rd Int. Conf. on Knowledge Discovery and Data Mining* pp 61–66
- Spensberger C, Madonna E, Boettcher M, Grams C M, Papritz L, Quinting J F, Röthlisberger M, Sprenger M and Zschenderlein P 2020 Dynamics of concurrent and sequential central European and Scandinavian heatwaves *Q. J. R. Meteorol. Soc.* **146** 2998–3013
- Spirtes P and Glymour C 1991 An algorithm for fast recovery of sparse causal graphs *Soc. Sci. Comput. Rev.* **9** 62–72
- Stefanon M, D'Andrea F and Drobinski P 2012 Heatwave classification over Europe and the mediterranean region *Environ. Res. Lett.* **7** 014023
- Suarez-Gutierrez L, Müller W A, Li C and Marotzke J 2020 Dynamical and thermodynamical drivers of variability in European summer heat extremes *Clim. Dyn.* **54** 4351–66
- Vautard R, Yiou P, D'Andrea F, de Noblet N, Viovy N, Cassou C, Polcher J, Ciais P, Kageyama M and Fan Y 2007 Summertime European heat and drought waves induced by wintertime mediterranean rainfall deficit *Geophys. Res. Lett.* **34** L07711
- Wang P, Tang J, Wang S, Dong X and Fang J 2018 Regional heatwaves in china: a cluster analysis *Clim. Dyn.* **50** 1901–17
- Wood R R and Ludwig R 2020 Analyzing internal variability and forced response of subdaily and daily extreme precipitation over Europe *Geophys. Res. Lett.* **47** e2020GL089300
- Wu X, Wang L, Yao R, Luo M and Li X 2021 Identifying the dominant driving factors of heat waves in the north china plain *Atmos. Res.* **252** 105458
- Zhuo W, Yao Y, Luo D, Simmonds I and Huang F 2022 Combined impact of the cold vortex and atmospheric blocking on cold outbreaks over east asia and the potential for short-range prediction of such occurrences *Environ. Res. Lett.* **17** 084037
- Zschenderlein P, Fink A H, Pfahl S and Wernli H 2019 Processes determining heat waves across different European climates *Q. J. R. Meteorol. Soc.* **145** 2973–89